Tellus SERIES A DYNAMIC METEOROLOGY AND OCEANOGRAPHY
PUBLISHED BY THE INTERNATIONAL METEOROLOGICAL INSTITUTE IN STOCKHOLM

Atypical anticlockwise internal tidal motions in the deep ocean

By HANS VAN HAREN*, *Royal Netherlands Institute for Sea Research (NIOZ), P.O. Box 59, NL-1790 AB Den Burg, the Netherlands*

(Manuscript received 25 February 2015; in final form 13 June 2015)

ABSTRACT

In the ocean, horizontal motions associated with freely propagating semidiurnal tidal inertia-gravity waves mainly describe an ellipse that is traversed in a clockwise direction in the Northern Hemisphere. In this article, rare observations of anticlockwise polarised semidiurnal motions are presented from deep North-Atlantic mooring sites. Anticlockwise motions are found to occur 1–20% of the time, irrespective of latitude and (weak) vertical density stratification. In a deep narrow channel like Kane Gap however, anticlockwise motions dominate over clockwise. The statistics of turbulence match the occurrence of polarisation change. It is unclear whether these observations represent theoretical predictions of reflected baroclinic Poincaré waves, or those involving the effects of the horizontal Coriolis parameter on internal wave propagation in weak stratification. The observed switching between clockwise and anticlockwise polarisation with time at a fixed position cannot be explained by the internal wave theory using the traditional approximation. Instead, the polarisation switching points at baroclinic effects involving varying background conditions like stratification and shear-induced mixing. It is suggested the polarisation statistics may be used as a diagnostic tool for such varying conditions.

Keywords: physical oceanography, deep-ocean current observations, internal wave motions

1. Introduction

Ocean interior observations by Leaman and Sanford (1975), Pinkel (1983) and van Haren (2006) showed relatively short vertical scales O (100 m) for near-inertial and tidal motions. They also showed a strong asymmetry in vertical propagation at particular sites where about 90% of the energy propagated down-/upward (as evaluated from phase propagating up-/downward), respectively. This strong vertical asymmetry not only suggested near-inertial motions generation near the surface (for buoyancy frequency $N > f$, f denoting the local inertial frequency) and internal tidal motions near the bottom but also strong absorption during propagation (St. Laurent and Garrett, 2002).

When data are examined in more detail, some time–vertical coordinate representations of band-pass filtered inertial motions have revealed rapid transitions in phase propagation, and even reversal in sign across thin layers O(10 m) in thickness, as mentioned by van Haren (2006). Thin layers were often accompanied by relatively large shear. As will be demonstrated in this article using long-term moored current meter observations, the reversal in sign of vertical–time phase propagation is a necessary condition for the rare switching of the polarisation direction, that is, of the sense in which a horizontal current ellipse is traversed in time of, specifically, semidiurnal tidal motions, the dominant internal wave motions.

One of the primary effects of the Earth rotation is (following, e.g., Gonella, 1972; LeBlond and Mysak, 1978) that at super-inertial frequencies horizontal motions in the ocean (perpendicular to gravity) traverse an ellipse path in an anticyclonic (clockwise in the Northern Hemisphere, NH) direction: they have exclusively clockwise 'polarisation' (and anticlockwise in the Southern Hemisphere). Examples are all types of free propagating Poincaré waves. Some theoretical exceptions exist. In the model of a rectangular basin closed at one end, the (infinite number of) reflected Poincaré waves have anticlockwise polarised motions in the NH (Taylor, 1922; Hutter et al., 2011). In the open-ocean inertia-gravity IG-wave domain, anticlockwise super-inertial motions are predicted for particular wave characteristics under relatively weakly stratified conditions (Gerkema and Exarchou, 2008). This prediction is made using 'non-traditional approximation' (non-TA), that is, by not using the traditional approximation (TA) of omitting the terms

*Correspondence
email: hans.van.haren@nioz.nl

Citation: Tellus A 2015, **67**, 27718, http://dx.doi.org/10.3402/tellusa.v67.27718

involving the horizontal Coriolis parameter in the equations of motions. Few observations exist of anticlockwise polarised motions, and notable exceptions are related with frictional effects on barotropic currents in shallow seas (e.g. Maas and van Haren, 1987).

The interest for studying potential anticlockwise internal tidal motions in the deep ocean comes from the importance of their mechanical energy input and shear for vertical turbulent mixing and variations with space and time therein. Due to the associated reduced vertical scales and relatively large energy content, their shear is important across interior density jumps of large stratification in thin layers. Ellipsoidal baroclinic internal wave motions may generate circular and rectilinear shear depending on slight changes in internal wave ellipticity or in their propagation direction, due to changes in stratification (van Haren, 2007). It is thus important to better understand the precise mechanisms behind vertical exchange, which is important for sediment and nutrient redistribution.

2. Vertical IG-wave polarisation theory

In a vertically (in situ) density stratified ocean, free internal waves exist at frequencies σ in the band $f<\sigma<N$ outside near-homogeneous waters, following the TA. Here, $f=2\Omega\sin\varphi$ indicates the local vertical component of the Earth's rotational vector $\mathbf{\Omega}$ at latitude φ.

In the non-TA approach, retaining also the horizontal component $f_h=2\Omega\cos\varphi$, IG-waves can be computed under an f-plane approximation and the IG-wave band extends beyond the TA-band above. Energy propagates along characteristics $\xi_\pm=\mu_\pm\chi-z$ in a plane (χ, z), where the horizontal coordinate $\chi=x\cos\alpha+y\sin\alpha$, α angle to East, so that (Badulin et al., 1991; Gerkema and Shrira, 2005),

$$\mu_\pm=\frac{ff_s\pm(f^2f_s^2+(\sigma^2-f^2)(N^2-\sigma^2+f_s^2))^{1/2}}{N^2-\sigma^2+f_s^2}, \qquad (1)$$

where $f_s=f_h\sin\alpha$.

In the case of only considering up- or downgoing characteristics, Gerkema and Exarchou (2008) find a simple expression for the ratio of minor to major axis or ellipticity of the horizontal (f-plane) current components u, v-hodograph,

$$|v|/|u|=|f_s\mu_\pm-f|/\sigma. \qquad (2)$$

This should be contrasted with the TA ellipticity result $|f|/\sigma$ and which fixes the polarisation per hemisphere (being strictly clockwise in the NH).

The sign of eq. (2) also determines the non-TA polarisation, which is clockwise when $f_s\mu_\pm<f$. Thus, anticlockwise near-inertial motions are predicted for the NH under particular non-TA conditions. These motions are separated from clockwise motions by the rectilinear motion condition $f=f_s\mu_\pm$, which reads using eq. (1),

$$\sigma=|f|N/(f^2+f_s^2)^{1/2}. \qquad (3)$$

For semidiurnal lunar tidal frequency $\sigma=M_2$ and meridional (North-South) propagation $\alpha=90^\circ$, eq. (3) yields for the transitional stratification in terms of buoyancy frequency,

$$N/2\Omega=M_2/f, \text{or } N=M_2/\sin\varphi \qquad (4)$$

Such weak stratification can be found in the deep ocean near the bottom mainly (Fig. 1). For observed typical weak near-bottom $N\approx 8\Omega$, the equality [eq. (4)] is expected to be found around latitude $\varphi=15^\circ$, so that dominant anticlockwise motions are predicted equatorward from this latitude (and clockwise motions poleward).

3. Data

We investigate data from about yearlong, deep moored current meters from locations across the tropical to mid-latitude Northeast Atlantic Ocean (Fig. 2). In open basins, instruments were about 500 metres above the bottom (mab), the deepest on 3–4 km long taut-wire moorings in 4–5 km water depths. At locations in the vicinity of topography as in the Bay of Biscay ($\sim$46°N), Kane Gap (KG, $\sim$9°N) and equatorial Romanche Fracture Zone (RFZ, $\sim$1°S),

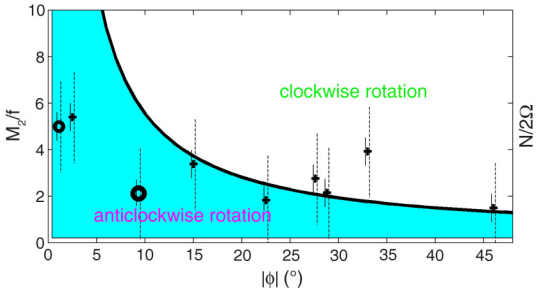

Fig. 1. Clockwise and anticlockwise polarisation of internal semidiurnal tidal waves as a function of latitude for given stratification. Theoretical curve [eq. (4)] following non-TA (see text) as a function of wave frequency ($\sigma=M_2$, lunar semidiurnal) scaled with the inertial frequency (heavy solid graph). The graph separates areas with dominant clockwise polarisation above it (white area) and anticlockwise polarisation below it (light-blue). The symbols represent mean local stratification in terms of buoyancy frequency computed over 100 m around the current meter depth and scaled with 2Ω (vertical solid lines indicate +/− one standard deviation; the thin dashed lines indicate the one std-extent of N over 10 m intervals, cf. van Haren and Millot, 2006). Observations are from: 500–1000 m above the 5000 m deep Atlantic Ocean abyssal plains (+) and about 100 m above the bottom (mab) in tropical channels (o) Kane Gap (KG) and Romanche Fracture Zone (RFZ). For locations, see Fig. 2.

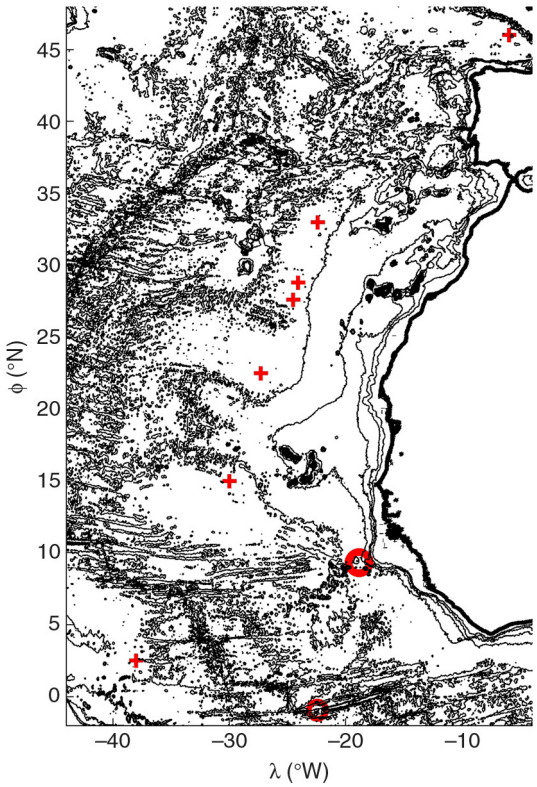

Fig. 2. Northeast Atlantic Ocean, mid-latitude-tropical region, with the positions of long-term mooring locations indicated by symbols. The seven open basin locations are indicated by crosses, the two channel locations by circles. Bathymetry is given every 1000 m from 0 to 5000 m.

instruments from about 100 mab were used on 1000, 200 and 350 m long cables, respectively. Using large buoyancy elements near their top, the moorings were designed to deflect minimally under local currents, with typical maximum speeds of $<0.25\,\mathrm{m\,s^{-1}}$. As a result, the deepest current meters moved less than 1 m in the vertical and 20 m in the horizontal. On the relatively short KG and RFZ moorings, the deflections were less than half those sizes. At the instruments' depths of some 4000 m, large (100-m) vertical scale stratification was generally weak, $N<10f$ or an internal wave bandwidth smaller than one order of magnitude, except near the equator (Fig. 1), as was established using 24-Hz sampling, $1\,\mathrm{m\,s^{-1}}$ lowering speed SeaBird 911-plus CTD-data obtained during the mooring deployment and recovery cruises. Referring to the error bars in Fig. 1 for N computed over 100 m (solid line) and 10 m (dashed line) vertical intervals, the accuracy of such CTD yields standard errors of about 1.2Ω and 4Ω in weakly stratified waters (van Haren and Millot, 2006).

The current meters were either acoustic Aanderaa RCM-9 or acoustic Nortek AquaDopp. They sampled at a rate of once per 900 s (15 min), with a few once per 600 s (10 min) for periods of at least 1 yr (one exception: RFZ, 6 months). This allowed full resolution of the entire IG-wave band. It also allowed a reasonably sharp separation of the dominant semidiurnal band from the rest of the spectrum using double elliptic filters (Fig. 3). As we investigate a particular IG-wave band, the semidiurnal (tidal) band, rather than a specific frequency, harmonic analysis is not opportune and a single set of fixed amplitudes and phases for these motions is not established. Instead, time series of band-filtered data are investigated.

The filter was applied to retain an approximate 10% wide semidiurnal band $D_2 = (0.95\ 1.05)M_2$ (20 dB reduction points), which is the typical internal tidal wave bandwidth (van Haren, 2004). Using filter design schemes from Parks and Burrus (1987), the phase preserving back-and-forth use of sharp elliptic filters with ripple correction showed less than 10^{-4} power remaining in the stop-bands and retained more than 0.99 of the power in the pass-band (Fig. 3). The choice of band-pass filter, including its width and other characteristics, is crucial for the polarisation results investigated here.

3.1. *Determination of polarisation*

To characterise the polarisation P in clockwise and counterclockwise directions using time series of band-pass filtered horizontal current data, their components [u(t), v(t)] are

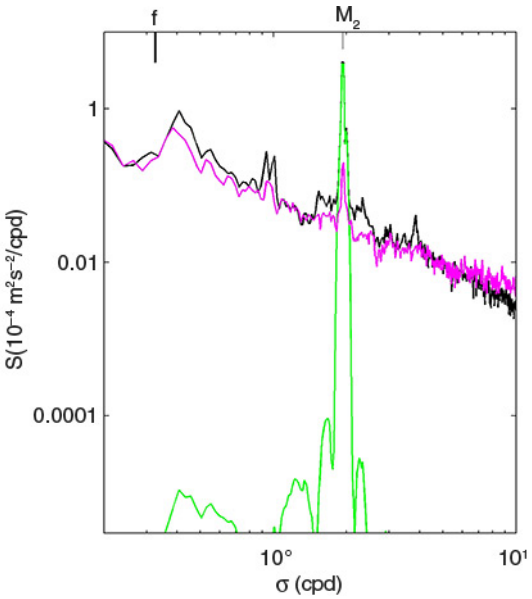

Fig. 3. Example of kinetic energy spectrum from a 1-yr current meter record at 105 mab in KG, including semidiurnal band-pass filter (green) and vertical difference spectrum from 5 to 210 mab (purple).

written as motions in a plane with real and imaginary axes (Gonella, 1972),

$$u - iv \approx Ae^{-i\sigma t}, \quad (5)$$

where A denotes a slowly varying amplitude, and $i^2 = -1$. The time variation of A is at a rate of one-tenth of the principal period or slower. In practice, this is accommodated here by the applied width of the band-pass filter. P is computed from the natural logarithm and time derivative of eq. (5),

$$P(t) = -i d\log(u - iv)/dt. \quad (6)$$

Its sign is negative for clockwise polarisation ($sgn P(t) < 0$; $C_-(t) = 1, C_+(t) = 0$) and positive for anticlockwise polarisation ($sgn P(t) > 0$; $C_+(t) = 1, C_-(t) = 0$). Here, we are only interested in the sign of the polarisation direction and not in the amplitude-phase modulation. For a single quantitative measure, we express the occurrence within a length of time of positive relative to the (TA-common) negative polarisation as the fraction,

$$R = \sum \{C_+/(C_- + C_+)\}, \quad (7)$$

summed over the entire time series. Thus, anticlockwise polarisation dominates when $R > 0.5$ and clockwise when $R < 0.5$. Note that this indicates a dominance as a function of time, which is not necessarily as a function of variance.

In order to compare eq. (7) with non-TA theory, not only 100 m large-scale N is computed, but also the statistical distribution of 10 m small-scale N_{10}. This is done by computing a fraction of occurrences of $N_{10} < M_2/\sin\varphi$ following eq. (4) over the total amount of local CTD-data points in the lower 600 mab.

4. Observations

Time series of P demonstrate that in the deep open Atlantic Basins semidiurnal motions are predominantly clockwise (negatively) polarised (Fig. 4a; example from 28.8°N in the CB). Below 4000 m, at about 500 mab, we observe $0.01 < R < 0.21$ (Fig. 1b; $2.5° < \varphi < 46°$N). The few anticlockwise motions (positive values in Fig. 4a) occur when the semidiurnal current amplitudes are relatively small (Fig. 4b). The corresponding hodographs (Fig. 5) are rather variable, describing either Lissajous figures or direction-invariant ellipse-widening and -thinning. Commonly, they exceed the instrumental noise level (light-blue circle). The pattern of motions designed in a 4-d hodograph during anticlockwise motion suggests a transition in phase propagation as across a (sheared) interface with the switch to clockwise motion via a rectilinear degenerated ellipse (Fig. 5a). This rare occurrence of anticlockwise polarisation is also found in time series of the difference between neighbouring current meters (500–700 m apart vertically; the motions represent reasonably high vertical-mode internal tidal waves), in the Bay of Biscay, the Cape Verde Basin, the equatorial Ceará Basin as well as in the near-inertial band (not shown).

In contrast, a rare predominantly anticlockwise semidiurnal motion is observed (Fig. 6a) at 105 mab near the sill of the 4560 m deep through-flow channel KG (Fig. 7). This anticlockwise semidiurnal dominance is observed in all three current meters records, although decreasing from $R = 0.89$ at 7 mab to $R = 0.61$ at 210 mab. In these records, anticlockwise motions occur also when current amplitudes are relatively large (e.g. Fig. 5b). It is noted that the rather weak and broadband near-inertial motions at this site are not predominantly anticlockwise polarised.

As the KG current meters were distributed over a 200-m-long cable holding 100 high-resolution temperature

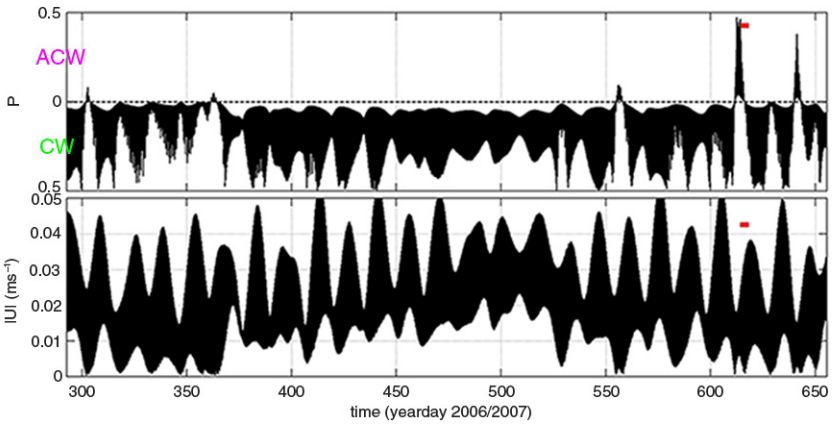

Fig. 4. One year time series of typical deep CB semidiurnal polarisation direction, observed at 28.8°N, 500 mab. The polarisation sign is anticlockwise when positive and clockwise when negative [arbitrary values between (−0.5, 0.5)]. The red bar indicates a 4-d period of which hodographs are given in Fig. 5a. (b) Current amplitude.

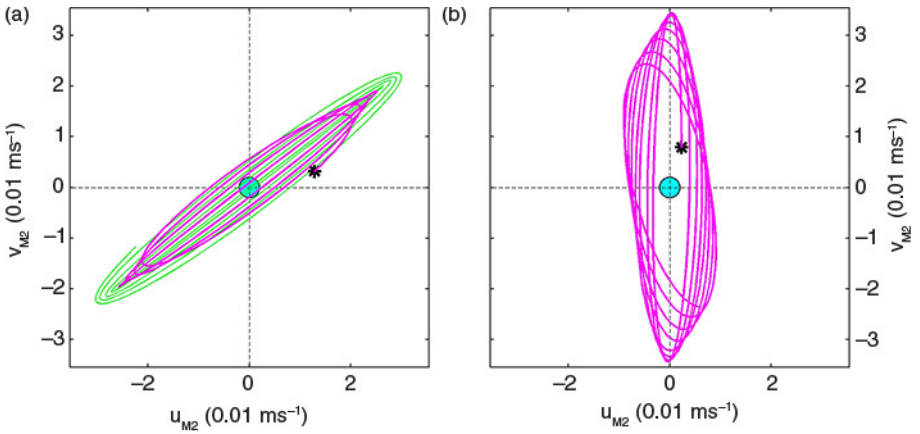

Fig. 5. Hodographs of 4 d of band-pass filtered semidiurnal motions. Green colours indicate clockwise motion, purple anticlockwise. Starting point is the star. The light-blue circle indicates the extent of one standard instrumental error. (a) CB, period indicated by small red bar in Fig. 4a. (b) KG, period indicated in Fig. 6a.

sensors, time series of vertical current shear $\mathbf{S}=[du/dz, dv/dz]$, stratification and the gradient Richardson number $Ri = N^2/|\mathbf{S}|^2$ could be computed over vertical scale of (at least) 100 m. This scale just resolves the largest vertical turbulent overturns (van Haren et al., 2013). At this vertical scale, portions of the time series of its inverse value 1/Ri (Fig. 6b) exceeding 1 ($Ri < 1$) reasonably resemble occurrences of anticlockwise polarisation. $Ri = 1$ is considered an (in)sufficient condition for (in)stability in nonlinear, 3D flows (Abarbanel et al., 1984). Although the precise phase relationship varies considerably, thereby reducing the correlation and pointing at distant besides local effects, the overall statistics correspond very well (Fig. 8, the red stars indicate fraction-$\{Ri < 1\}$). The time-scales of variation of 4–50 d between switching and Ri-variations also correspond well. This was also found for recent data from the RFZ, where polarisation is just predominantly anticlockwise.

Statistics of the fraction-$\{N_{10} < M_2/\sin\varphi\}$ as in eq. (4) using small (10 m vertical) scale stratification (Fig. 8) from CTD-data basically follow the distribution of large-scale $N < M_2/\sin\varphi$ (Fig. 1) with latitude. Following non-TA theory, they predict dominant anticlockwise semidiurnal motions in the tropics ($0 < \varphi < 23.5°N$) and clockwise motions in the subtropics ($23.5 < \varphi < 45°N$). However, in the tropics, dominant anticlockwise motions were found in turbulent deep narrow channels only, not in open basins (current meters at four more moorings in the Ceará Basin showed the same low R as at 2.5°N in Fig. 8). Thus, a simple relationship between P(t) and (N, φ)(t) is not found, whereas the correspondence R and the 'mixing statistics' of the fraction-$\{Ri < 1\}$ are established for the few high-resolution data sets available.

5. Discussion

In comparison with the near-rectilinear inertial horizontal motions observed in the deep Mediterranean (van Haren and Millot, 2004), the present effects of polarisation change in tropical deep-ocean internal tidal motions provide a slightly ambiguous proof of the non-TA influence of the

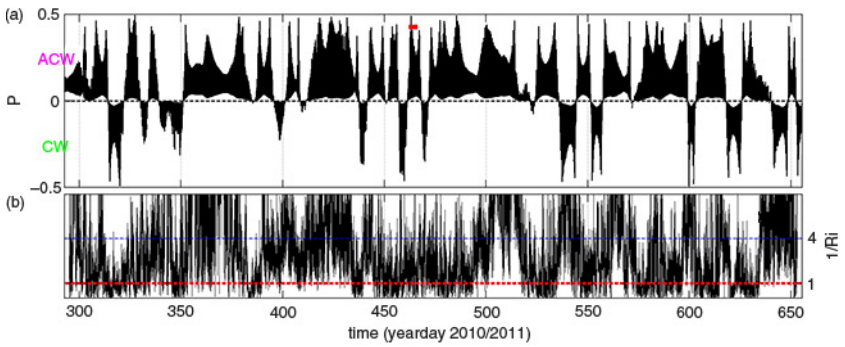

Fig. 6. As Fig. 4, but for observations at 105 mab in KG in panel a. (b) Inverse of local gradient Richardson number, computed from high-resolution temperature observations and current meter records.

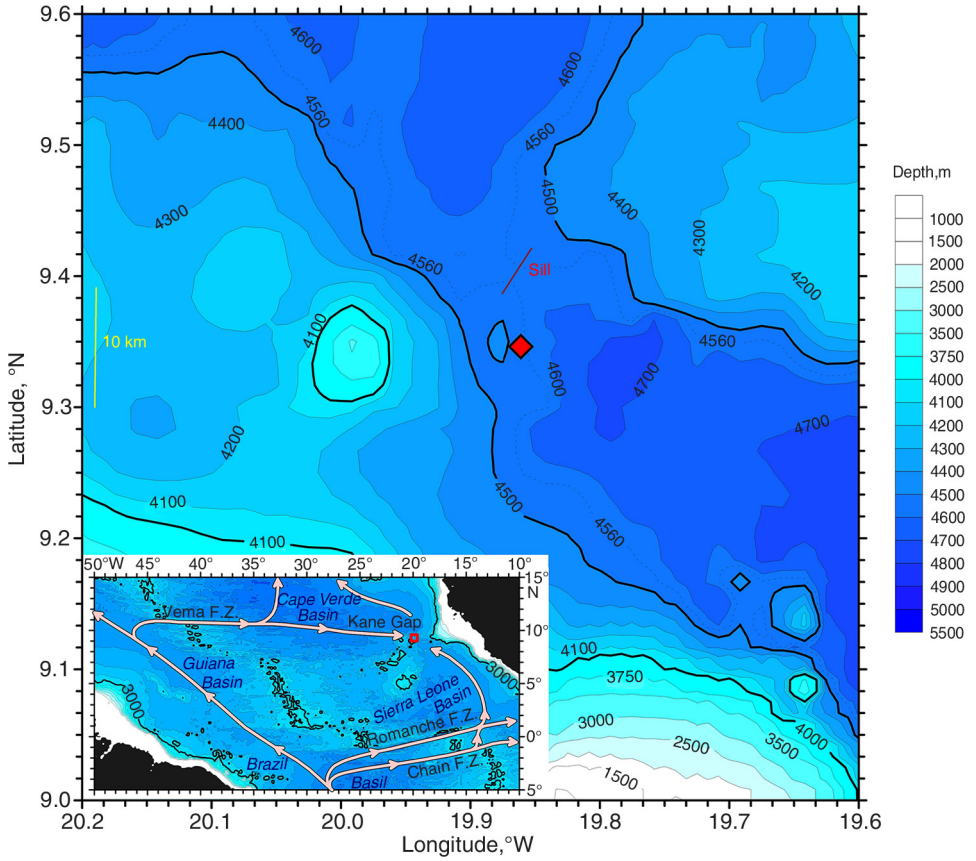

Fig. 7. Mooring location in KG, a varying through-flow of Antarctic Bottom Water in the eastern tropical Atlantic (insert). The mooring was about 5 km south of the main sill, just east of a small (<100 m high) hill.

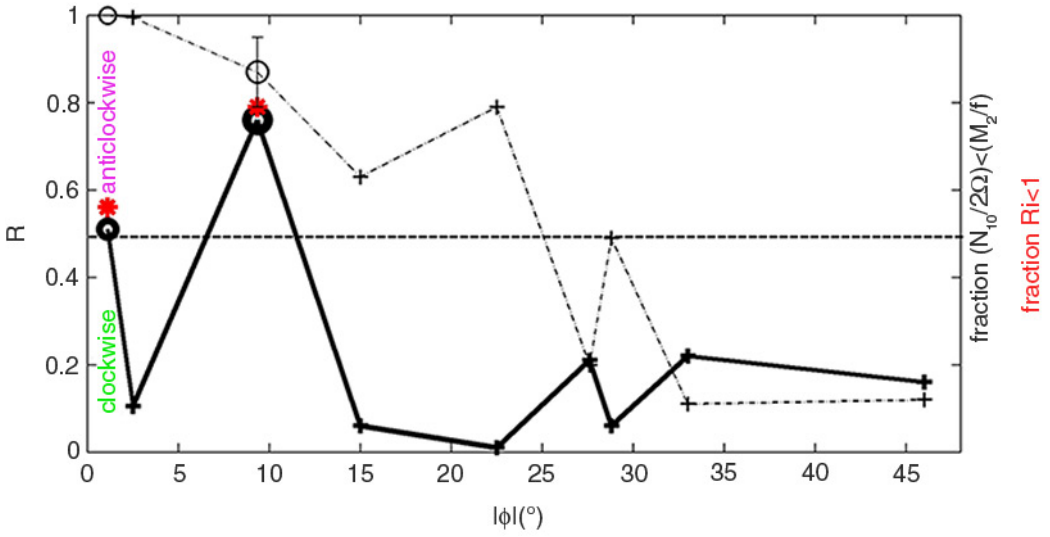

Fig. 8. Fraction of anticlockwise polarisation from yearlong current meter records (heavy solid line and symbols) compared with the fraction (statistics) of 10-m scale buoyancy frequency below the local theoretical threshold in eq. (4) of the wave frequency/sin(φ) (thin dash–dotted line and symbols). For the latter, an estimate of the standard error is given by the vertical line for the KG-data. Statistics are built over an equivalent range of 600 m around the current meter depths, commonly distributed over three profiles near the moorings.

Earth rotation in weakly stratified waters, even though TA predicts exclusively clockwise internal wave motions in the NH. On the one hand, the observations of dominant anticlockwise motions in tropical KG and equatorial, hence complex, RFZ, and the dominant clockwise motions at subtropical latitudes confirm proposed non-TA theory (Gerkema and Exarchou, 2008). On the other hand, we find several discrepancies between observations and non-TA theory, in the Cape Verde and Ceará basins. Apparently, the non-TA-inspired parameterisation [eqs. (2)–(4)] using N (and a hypothetical constant $|\mathbf{S}|$) is insufficient for a description of dominant anticlockwise polarisation in open-ocean basins. We also note that none of the investigated time series shows exclusive (100% pure) clockwise, or anticlockwise, polarisation, although this may be mere coincidence as half-year long periods of unique (clockwise) polarisation have been observed (cf., days 360–550, Fig. 4a).

The assumption underlying the (theoretical) prediction of anticlockwise polarisation of super-inertial IG motions in the NH involves wave propagation in one vertical direction, up or down, only. This assumption may not be realistic, especially in the open ocean far from boundaries, where waves from many sources combine and large vertical scale motions are considered to dominate (St. Laurent and Garrett, 2002). In the vicinity of the main source of internal tides near the top of continental slopes and large seamounts, this would be a downgoing beam of wave energy (e.g. Pingree and New, 1990). In those waters relatively close to the surface however, N is too large for non-TA effects to be important. Near deep topography like relatively small hills and channels but also above ridges like the Reykjanes, this would be an upgoing beam (van Haren, 2006). Over such deep topography and relatively close to the equator, N can be sufficiently small for non-TA to take effect.

It is quite clear that the present time series observations of varying polarisation, switching between clockwise and anticlockwise, cannot be explained from internal wave theory invoking TA that predicts exclusive clockwise polarisation in the NH for super-inertial motions. It is also clear that the observations do not describe barotropic motions of reflected Poincaré waves that would also not change polarisation with time. The latter is not too surprising as the (external) Rossby radius of deformation is larger than 2000 km in the deep ocean, so that its area of influence away from major topography would affect all abyssal basins, which is not observed.

The present observations, thus, represent baroclinic motions and are subject to any variations with time of the background conditions stratification and turbulent mixing, mainly caused by shear and convection. Such variations may be local, but can also be inflicted remotely, thereby causing a local variation in a wave's pathway. Variation with time of background conditions may also affect the location of an internal wave source.

As deep channels are narrow conduits with topography nearby, they are considered as potential internal wave source and an area with relatively high levels of turbulent mixing due to strong currents, albeit with overall weak stratification. They are, thus, ideal for non-TA effects, as is represented here by the statistics of variation in mixing in terms of the gradient Richardson number. The geometry of the mooring location near a sill of the channel cannot rule out the set-up of reflected baroclinic Poincaré waves as the internal Rossby radius is estimated to be between 0.5 and 10 km, depending on the vertical scale used. In the KG, the mooring is located 5 km south of the main sill and about 1 km from a small hill (Fig. 7). However, even if this process were important here, the reflected Poincaré waves are not found exclusively anticlockwise polarised. Such a switch in polarisation is not described by Taylor's (1922) theory.

As the present observations at least statistically show reasonable correspondence with background conditions, especially turbulence levels in terms of the inverse gradient Richardson number, it is tempting to formulate a diagnostic use for the polarisation. After all, moored current meter observations are amongst the easiest to make in oceanography. As polarisation of propagating waves is not only dependent on local conditions and variations therein, the proposed best use is statistics, as precise phase relationships within a time series are hard to establish.

6. Conclusion

We have presented fairly unique anticlockwise polarised deep-ocean semidiurnal tidal motions. They are found at all the North-Atlantic Ocean sites investigated here, while generally over brief periods of time compared to dominant clockwise polarisation. In tropical deep channels however, motions are found dominantly anticlockwise polarised. This dominance is coincident with low Richardson number, high turbulence conditions, in generally weakly stratified waters. The switching between clockwise and anticlockwise motions thus reflects the (time-scale of) variations in background conditions affecting the density-driven baroclinic motions. The present effects of polarisation change in tropical deep-ocean internal tidal currents provide further proof of the influence of the Earth rotation in weakly stratified waters, although wall-effects of reflected waves cannot be ruled-out from the single mooring observations.

7. Acknowledgements

I thank the crew of the R/V Pelagia for deployment and recovery of the moorings. NIOZ-MTM helped preparing moorings and instrumentation. I thank L. Maas and T. Gerkema for discussions on polarisation matters and R. Tarakanov for preparing Fig. 7. Large investment budget

'LOCO' and Russia–Netherlands collaboration program 'RUSNL' were financially supported in part by the Netherlands Organization for the Advancement of Scientific Research, NWO.

References

Abarbanel, H. D. I., Holm, D. D., Marsden, J. E. and Ratiu, T. 1984. Richardson number criterion for the nonlinear stability of three-dimensional stratified flow. *Phys. Rev. Lett*. **52**, 2352–2355.

Badulin, S. I., Vasilenko, V. M. and Yaremchuk, M. I. 1991. Interpretation of quasi-inertial motions using Megapoligon data as an example. *Izv. Atmos. Oceanic Phys*. **27**, 446–452.

Gerkema, T. and Exarchou, E. 2008. Internal-wave properties in weakly stratified layers. *J. Mar. Res*. **66**, 617–644.

Gerkema, T. and Shrira, V. I. 2005. Near-inertial waves in the ocean: beyond the 'traditional approximation'. *J. Fluid Mech*. **529**, 195–219.

Gonella, J. 1972. A rotary-component method for analyzing meteorological and oceanographic vector time series. *Deep Sea Res*. **19**, 833–846.

Hutter, K., Wang, Y. and Churabenko, I. P. 2011. *Physics of Lakes. Vol 2: Lakes as Oscillators*. Springer, Berlin, 646 pp.

Leaman, K. D. and Sanford, T. B. 1975. Vertical propagation of inertial waves: a vector spectral analysis of velocity profiles. *J. Geophys. Res*. **80**, 1975–1978.

LeBlond, P. H. and Mysak, L. A. 1978. *Waves in the Ocean*. Elsevier, Amsterdam, 602 pp.

Maas, L. R. M. and van Haren, J. J. M. 1987. Observations on the vertical structure of tidal and inertial currents in the central North Sea. *J. Mar. Res*. **45**, 293–318.

Parks, T. W. and Burrus, C. S. 1987. *Digital Filter Design*. Wiley, New York, 342 pp.

Pingree, R. D. and New, A. L. 1990. Downward propagation of internal tidal energy into the Bay of Biscay. *Deep Sea Res. A*. **36**, 735–758.

Pinkel, R. 1983. Doppler sonar observations of internal waves: wave-field structure. *J. Phys. Oceanogr*. **13**, 804–815.

St. Laurent, L. and Garrett, C. 2002. The role of internal tides in mixing the deep ocean. *J. Phys. Oceanogr*. **32**, 2882–2899.

Taylor, G. I. 1922. Tidal oscillations in gulfs and rectangular basins. *Proc. Lond. Math. Soc*. **s2–XX**, 148–181.

van Haren, H. 2004. Bandwidth similarity at inertial and tidal frequencies in kinetic energy spectra from the Bay of Biscay. *Deep Sea Res. I*. **51**, 637–652.

van Haren, H. 2006. Asymmetric vertical internal wave propagation. *Geophys. Res. Lett*. **33**, L06618. DOI: 10.1029/2005GL025499.

van Haren, H. 2007. Inertial and tidal shear variability above Reykjanes Ridge. *Deep Sea. Res. I*. **54**, 856–870.

van Haren, H. and Millot, C. 2004. Rectilinear and circular inertial motions in the Western Mediterranean Sea. *Deep Sea Res. I*. **51**, 1441–1455.

van Haren, H. and Millot, C. 2006. Determination of buoyancy frequency in weakly stable waters. *J. Geophys. Res*. **111**, C03014. DOI: 10.1029/2005JC003065.

van Haren, H., Morozov, E., Gostiaux, L. and Tarakanov, R. 2013. Convective and shear-induced turbulence in the deep Kane Gap. *J. Geophys. Res*. **118**, 5924–5930. DOI: 10.1002/2013JC 009282.